Journal of Cleaner Production 346 (2022) 131110

Contents lists available at ScienceDirect

Journal of Cleaner Production

journal homepage: www.elsevier.com/locate/jclepro

Optimizing demand response of a modular water reuse system in a remote Arctic microgrid

Daniel J. Sambor [a,*], Samantha C.M. Bishop [a], Aaron Dotson [b], Srijan Aggarwal [c], Mark Z. Jacobson [a]

[a] Department of Civil and Environmental Engineering, Stanford University, 473 Via Ortega, Stanford, CA, 94305, USA
[b] Civil Engineering Department, College of Engineering, University of Alaska Anchorage, 3211 Providence Dr, Anchorage, AK, 99508, USA
[c] Department of Civil, Geological and Environmental Engineering, College of Engineering and Mines, University of Alaska Fairbanks, PO Box 755915, Fairbanks, AK, 99775, USA

ARTICLE INFO

Handling Editor: Kathleen Aviso

Keywords:
Microgrid
Renewable energy
Dispatchable loads
Demand-side management

ABSTRACT

Reliance on imported diesel fuel, with high transportation costs, has made power and water treatment expensive in remote diesel microgrids in the Arctic. Past attempts at implementing piped water in these areas have proven difficult due to the high cost of energy to pump, transport, and heat water with imported diesel fuel. A modular Water Reuse (WR) system has been developed to provide more affordable, distributed water service for an individual home lacking running water. However, these WR systems still consume substantial electricity and can burden a household with high energy costs, if powered by the community diesel microgrid. Here we expand a mixed-integer linear optimization model — Food-Energy-Water Microgrid Optimization with Renewable Energy (FEWMORE) — to treat the effects of operating WR systems as dispatchable loads connected to a microgrid. We apply the model to a western Alaska community without piped water to analyze demand response (DR) of WR systems with solar and wind energy. Such an analysis has not yet been articulated by current energy optimization, water treatment, and demand response models for modular water service in microgrids. Integrating a solar photovoltaics (PV) array to power a WR system, as opposed to operating solely off of diesel generation, results in a 3% decrease in total project costs (installing and maintaining solar PV, and electricity purchases from the diesel microgrid) over a 20-year lifetime. Optimally dispatching the water treatment processes results in more savings: a 13% decrease in total project costs and a 37% reduction in diesel use.

1. Introduction

In rural Alaska communities, electricity generation is expensive, up to $1/kWh, compared with the average U.S. rate of $0.13/kWh (Alaska Energy Authority, 2019; U.S. Energy Information Administration, 2020). These communities are not connected to the state and continental electric grids and thus function as islanded microgrids, or self-sufficient, isolated electric delivery systems. They must each operate diesel generator powerhouses to supply electricity. However, about 200 communities are not connected to the state road system, so diesel must be shipped in via barge or plane at high cost (Holdmann et al., 2019). Local renewable energy, which could include solar PV and wind turbines, may provide more cost-effective and resilient electricity generation in these areas.

Meanwhile, drinking water is also an insecure commodity in remote Alaska communities (Eichelberger, 2010). In rural Alaska, over 4000 households across 30 communities do not have in-home piped drinking water or wastewater services due to high transportation, capital, installation, and maintenance costs of developing infrastructure (United States Arctic Research Commission Alaska Rural Water and Sanitation Working Group, 2015). Typical solutions, such as residential well and septic systems, are often infeasible due to risk of damage from permafrost thaw and associated high costs (Hennessy and Bressler, 2016). In lieu of piping infrastructure, community members must use a central location, called a washeteria, to purchase and haul water, take showers, and do laundry (Penn et al., 2017). Washeterias use substantial energy for water pumping, treatment, and heating (Rashedin et al., 2020). Thus, the high cost and time investment of hauling water have resulted in low water usage rates by community members and increased risk of illnesses stemming from poor sanitation (Eichelberger, 2010; Hennessy et al.,

* Corresponding author.
E-mail address: dsambor@stanford.edu (D.J. Sambor).

https://doi.org/10.1016/j.jclepro.2022.131110
Received 18 October 2021; Received in revised form 1 February 2022; Accepted 22 February 2022
Available online 26 February 2022

2008).

Analogous to distributed energy resources like solar PV, modular water recycling systems integrated with residences may provide more affordable, reliable, and secure methods of water delivery (Hickel et al., 2018). Such a technology, the WR system, has been developed at the University of Alaska Anchorage (UAA) (Hickel et al., 2018). The WR system is unique in its ability to be easily integrated, compared to traditional piped water infrastructure, as a shipping container unit next to homes in remote arctic climates. However, operating these WR systems can require substantial user cost for operation and maintenance, not including electrical or heating costs of each water fixture (Dotson, 2017). The community's desire for water services and acceptance of user rates are described in depth in Lucas et al. (2021). Integrating renewables to replace some diesel fuel to power these WR systems may reduce operating costs.

Additionally, if the WR systems can operate at times of excess renewable electricity generation (beyond the electricity used for typical loads), they can essentially be powered for free. For example, if there are high winds, and existing wind turbines are generating excess electricity, then the WR systems could use the excess electricity to treat/heat water. When the wind is not blowing, the WR systems would function at lower power levels, by only distributing treated water and collecting wastewater. Thus, dependence on battery storage can hypothetically be reduced by effectively storing energy in the form of treated/heated water. The WR systems are unique compared to traditional water treatment plants in that their processes can, in theory, be more easily controlled to run on renewable energy, given their distributed nature.

Optimally managing the operation of electric loads is termed demand-side management (DSM), which encompasses DR, or flexible load shaping (Pina et al., 2012; Jabir et al., 2018). There are numerous models for analyzing energy systems at a variety of scales (Quitoras et al., 2020; Quitoras, 2020; Khan et al., 2021; Zia et al., 2018) and many utilizing DSM (Rezaei and Kalantar, 2015; Moura and De Almeida, 2010; Aghajani et al., 2017); however, a common limitation is that specific load sectors and technologies are not considered (Jabir et al., 2018). Instead, many models assume a general percentage of load eligible for DSM without referencing its application and implementation. This study aims to apply DSM to the water sector, which is also well represented in the energy-water nexus literature, though mostly in larger-scale water systems (Pourmousavi et al., 2014; Kirchem et al., 2020; Soshinskaya et al., 2014; Zohrabian and Sanders, 2020).

However, upon review of DSM models in the water sector, most either generalize the electric loads of treatment plants and aggregate their ability to provide DSM benefits to the electric grid (Moura and de Almeida, 2010; Kirchem et al., 2020; Neves et al., 2015) or analyze treatment processes with sophisticated detail, but without assessing how their DSM potential can improve grid stability (Kirchem et al., 2020). The former, termed energy system models, use common linear programming (LP) or mixed-integer linear programming (MILP) optimization techniques to analyze the impact of water treatment DSM on the grid. The latter, called process optimization and simulation models, simulate the inner processes of the water treatment plants in high detail using non-linear programming methods; however, the computational complexity of water process modeling limits their ability to analyze the impact of water treatment DSM potential on broader electric grid operations (Kirchem et al., 2020; Soshinskaya et al., 2014).

According to a comprehensive review paper, Kirchem et al., 2020, on DSM within the energy-water nexus, "an integrated energy system should ideally incorporate both the relevant details of a process model and the power system to capture the potential for DR from a system perspective (Kirchem et al., 2020)." However, Kirchem et al. state that "this literature review has shown that there is not yet a model which combines these two important aspects to perform a meaningful analysis of the DR potential from industrial processes such as WWTPs (wastewater treatment plants) (Kirchem et al., 2020)." No studies have quantified DSM potential of small-scale water reuse systems and the subsequent effect of water treatment process DSM on renewable energy capacity planning and dispatch optimization in islanded microgrids (Kirchem et al., 2020).

The contribution of this paper is the development and application of a tool, FEWMORE, that can model both the DSM potential of water treatment processes in a novel WR system, and its impact on energy optimization within an islanded renewable microgrid. FEWMORE optimizes the capacity and operations of solar PV and battery storage, and dispatch of excess generation from existing wind capacity, in order to power optimally-controlled water treatment/heating processes in a WR system. FEWMORE has previously been applied to a containerized growing system to optimize dispatch of ventilation, dehumidification, and lighting with renewable energy in a microgrid (Sambor et al., 2020). In this paper, the WR system is introduced, methods for modeling renewable integration and DSM of the WR system are described, and results are discussed. The goal of the paper is to inform energy and water-insecure communities how to optimally integrate WR systems with renewable energy in their microgrids to provide lowest-cost water treatment, while ensuring treatment processes still provide satisfactory sanitation services.

2. Methods

2.1. Water reuse system overview

The WR system, developed at UAA and described previously (Hickel et al., 2018; Lucas et al., 2021), addresses aforementioned challenges in rural water delivery. The WR system is housed in a shipping container (see Appendix A), connected to a single home via water supply and return lines. It can be divided into two different subsystems: the wash-water system (Fig. 1), which treats and recycles greywater from household fixtures via water treatment processes and other supporting technologies; and the heating system, which heats water and the container. The wash-water system consists of pre-treatment with cartridge filtration (CF), nano-filtration (NF), and reverse osmosis (RO), as well as ultraviolet (UV) lamps and ozone for disinfection. In this study, greywater is composed of four sources: shower, bathroom sink, kitchen sink, and laundry.

First, greywater enters the WR system and passes through a screen. It is then pre-treated by a series of cartridge filters (sizes 1 μm, 0.45 μm, and 0.2 μm). Next, water is treated sequentially by NF and RO operating in batch concentration mode (Hickel et al., 2018). Computer-controlled, actuated valves allow the piping to be interconnected so the primary pump (1.5 HP rotary vane) feeds each process. After these filtration steps, the water is disinfected using two UV contact lamps, each providing at least 5.5-log removal for viruses (Michaelson, 2017). The final treated water is sent to the wash-water tank, which stores clean water for domestic use. Post-treatment disinfection is performed by an ozone-generating UV light periodically in the wash-water tank to maintain water quality and avoid use of a chemical disinfectant (see Appendix E). The effects of backwashing of filters, varying greywater pollution load, and system flushing with additional make-up water are also part of system operation, but are not modeled.

2.2. Water use demand

In a rural Alaska community practicing self-haul, residents use on average 9 L of water per person per day (Eichelberger et al., 2020) for drinking, cooking, washing, cleaning, and waste processing. This is lower than the World Health Organization's recommended 50 L/person/day, and significantly lower than the United States average of 310 L/person/day (Dieter et al., 2018). The WR system is designed to provide 227 L/day (60 gal/day) for a household of four people.

Water use data were collected from a WR system prototype over a two-year period in Anchorage, AK (July 2016–June 2018), using water use guidelines as well as greywater and operational conditions provided

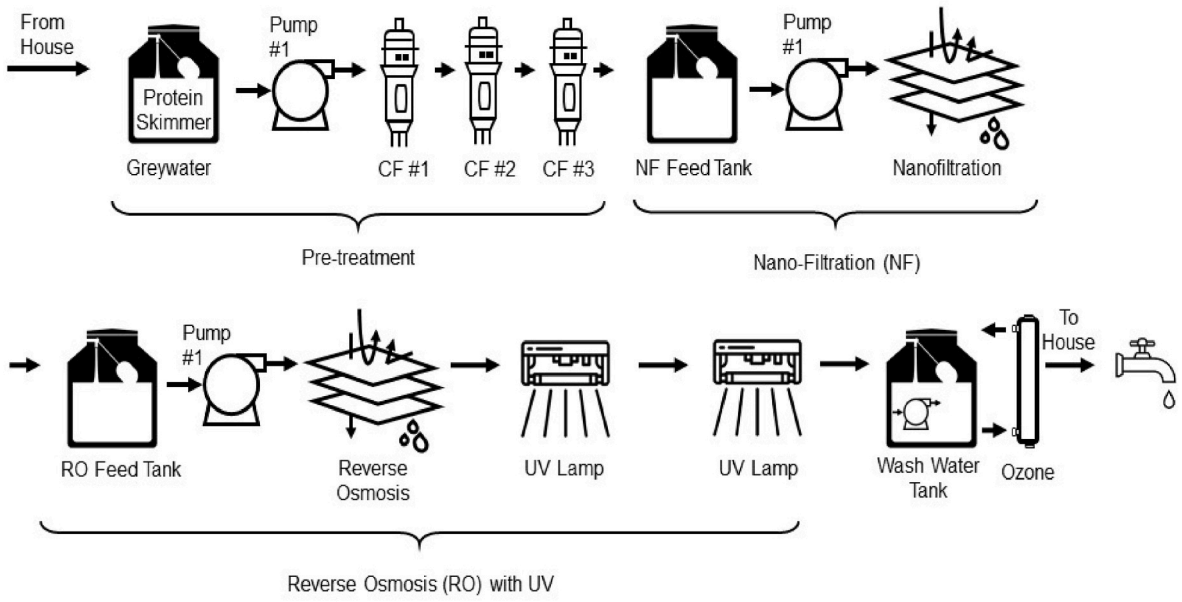

Fig. 1. Wash-water system process flow including greywater collection, three treatment processes, and return of treated water back to the house for domestic use.

by NSF 350 (NSF International, 2019). Two weeks of hourly data (April 18 - May 2, 2017) were selected, processed, and extrapolated to form a full year; this provided a consistent profile independent of prototype maintenance shutdowns. All challenge tests, outliers, and incomplete data were excluded. Regular loading periods were isolated to determine periods of "regular use" where influent quality varied and membrane operating pressure reflected average pumping pressure requirements over its lifetime. Data were selected so as not to favor best-case scenario conditions, such as relatively new membranes operating at high flux.

A selected day of domestic water use by application is shown in Fig. 2. Showering consumes approximately 79.5 L/day; the kitchen sink uses 37.9 L/day; the bathroom sink uses 53 L/day; and 1 load of laundry (57 L/load) is performed per day (Lucas et al., 2021). There are two diurnal peaks of water use, a morning peak and evening peak—typical of municipal water treatment facilities (Michaelson, 2017; Emami et al., 2018). Changes in water use or operation of domestic water fixtures, different than the given domestic water use profile, are not considered.

2.3. WR system power use

Existing power data of the WR system were processed similar to water use data. Energy use data can be categorized by the wash-water treatment processes (CF, NF, and RO) and supporting processes. Power and energy use are shown in Table 1. Power requirements result

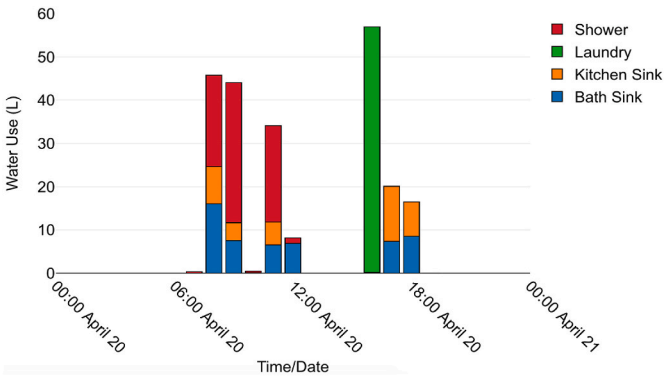

Fig. 2. Water use profile based on a representative day (April 20, 2017) of prototype testing.

Table 1
All electrical loads of the Water Reuse (WR) system, including a wash-water system for treating water, and a heating system for heating water and the container.

Category	Component	Power (kW)	Annual Energy (kWh/yr)	Daily Energy (kWh/day)
Wash Water: Main Processes	CF	0.36	422	1.16
	NF	0.34		
	RO	0.42		
Wash Water: Supporting Processes	UV	0.07	469	1.28
	Post-treatment	0.06		
	Valves/Misc	0.06		
Wash Water: Supplementary	Compressor	0.02	264	0.71
	Battery	0.01	55	0.15
	Fans/Misc	0.005	23	0.06
Heating	Space Heater	1	846	2.3
	Hot Water Heater	1.5	930	2.5

in the following treatment rates: CF treats 265 L/h, NF provides 246 L/h, and RO processes 159 L/h. This translates to an energy ratio of 0.37 kWh/m^3 for CF; 1.3 kWh/m^3 for NF; 2.9 kWh/m^3 for RO, including UV; and a total of 4.62 kWh/m^3. This is high compared with 0.5–2 kWh/m^3 for municipal wastewater treatment and recovery in the literature (Gude, 2015), which is dominated by pumping loads (Kirchem et al., 2020). In terms of power use over time, most processes exhibit constant power use except for RO, which has parabolic power use per cycle. RO power decreases as the water is warmed by the pump and then increases as concentration increases or the membrane fouls; the model has been weighted appropriately (see Appendix D).

Additional treatment processes (called "supporting processes" here) include UV, post-treatment (ozone), and valves, with power and energy use also shown in Table 1. There are also supplementary processes (with relatively small power use) including a compressor to collect greywater from the house; a battery to supply power to DC pumping loads for treated water distribution; and fans. When treatment processes are modeled as dispatchable loads (see Sec. 3.2), an additional 10 W is added to account for sensing. The entire wash-water system, within the WR system, uses 2.4 kWh/day, which is relatively consistent throughout prototype operation. A time series of energy use by component over a

typical day is shown in Fig. 3.

The WR system also must heat water for domestic hot water use. Data were not collected on thermal energy use during prototype operation; thus, heating processes have been modeled (see Sec. 2.4.2). In the prototype there are four small hot water tanks: two 15-L (4-gal) tanks and two 9.5-L (2.5-gal) tanks. For modeling simplicity, these are aggregated into a larger 50-L capacity hot water tank. Hot water demand is assumed to be 15 L per shower and per laundry load, and one-third of all water use in the bathroom and kitchen sinks.

A heating system is included in the shipping container for periods of cold weather. An electric resistance space heater is used and set to 10 °C (50 °F). Internal gains from pumping equipment, warm water returning from the home, and standby heat loss from water tanks provide additional heat.

An experimental diagram of all sub-systems of the WR system is shown in Fig. 4. Typically in studies analyzing DSM, a control case with no DSM (referred to here as Base Case) is compared with using DSM (Dispatchability Case) to analyze the effect of controlling, or dispatching, loads (Pina et al., 2012). In the case of the WR system, the three treatment processes (CF, NF, and RO) and the two heating processes (hot water and space heating) are considered dispatchable. The DSM strategy of load shifting is utilized for the purposes of intermittent renewable energy integration. For example, the WR system has to treat and heat a specific amount of water over a diurnal period; as long as system constraints are met (tank capacities, water temperatures, and minimum treatment processing time; see Sec. 2.4.1), water treatment and heating schedules can be shifted according to renewable resource availability.

The three main treatment processes and heating systems are chosen for dispatchability given their flexibility does not compromise the entire WR system's operation. The treatment processes can be dispatched asynchronously, because each has a preceding feed tank for storing water for treatment. Granted, some sub-processes within treatment and distribution may not shut down completely, and a small battery is already included within the container to accommodate. Water treatment processes and heating systems are also the sub-systems with the highest proportion of system electricity use.

2.4. FEWMORE model

The FEWMORE model is an MILP energy optimization model developed in Julia/JUMP (Version 1.1.0) (Dunning et al., 2017) at an hourly temporal resolution. The model inputs hourly annual profiles of WR system electric demand, domestic water demand, solar resource, wind generation, and temperature, assuming perfect forecast (see Appendix A).

The model optimizes three groups of decision variables (up to 13 total variables): 1) capacity of solar PV and battery system (lithium-ion battery and battery inverter) infrastructure to install; 2) hourly dispatch of energy generation (solar energy to curtail, wind energy to absorb from existing array, and diesel generation to purchase from microgrid), and battery storage (charging and discharging, with associated state-of-charge); and 3) hourly dispatch of water treatment processes (amount of water to treat per CF, NF, and RO cycle, with associated feed tank levels), and heating processes (amount of heat to hot water tank and container, with associated thermostat settings).

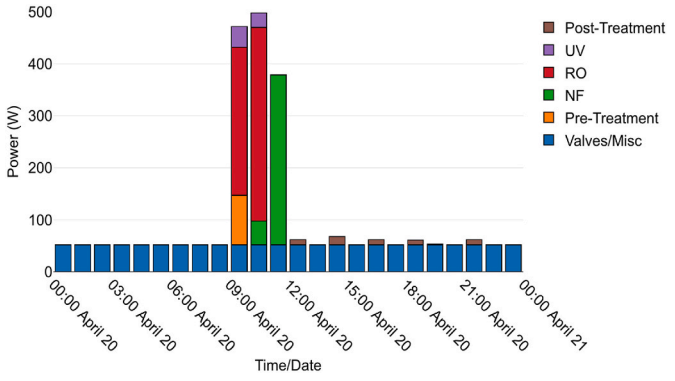

Fig. 3. Power use of wash-water system components for a representative day of prototype testing (April 20, 2017).

The model objective is to minimize total lifetime cost associated with powering a WR system over its 20-year project lifetime, in present dollars (Equation (1)). Costs can be grouped into three categories: 1) capital and installation cost of solar PV and battery; 2) annual operation and maintenance cost of solar PV and battery; and 3) annual cost of purchasing electricity from the diesel microgrid in each hourly time step, *t*. The costs are extrapolated to the total lifetime via a discounted cash flow analysis, with a real discount rate of 3% and grid escalation rate of 3%. Costs of operating and maintaining the existing diesel generator and wind array are beyond the scope.

$$\min \Sigma_t \, C_g{*}G_t + S{*}C_s + C_E{*}E + C_I{*}I \tag{1}$$

All costs, C, can be divided by component, where g is grid electricity, s is solar PV array capacity, E is the battery energy storage capacity, and I is the inverter capacity.

In addition to constraints on the wash-water system (Sec. 2.4.1) and heating system (2.4.2), all energy conversion among generation (diesel generator G, solar PV supplied S or curtailed R, storage (battery E), and demand technologies (l) must be balanced in each time step (Equation (2)).

$$G_t + S_t + W_t + E_{out,t} = l_t + E_{in,t} + R_t \tag{2}$$

Battery storage charging (E_{in}) and discharging (E_{out}) must be constrained with regard to available storage energy and power constraints, by tracking battery storage (SE) (Equation (3)).

$$SE_{t+1} = SD{*}[c{*}E_{in,t} - (1/d){*} + E_{out,t}] \tag{3}$$

The charging (c) and discharging (d) efficiencies result in a round-trip efficiency of 90% and the self-discharge rate (SD) is 0.01%/hr.

Solar PV and battery capacity can be installed on or proximate to the WR container connected to the home, similar to a typical residential grid-connected solar PV array (see Appendix F). Solar PV, battery storage, and battery inverter capital and installation costs are assumed to be $4500/kW, $1000/kWh, and $1000/kW, respectively (see Sec. 3.2.7 and Appendix A).

In order to mitigate potential complications of renewable integration, excess solar generation (beyond WR system demand or exceeding battery capacity) is curtailed. Thus, remaining system demand is met by diesel or wind from the community microgrid. Diesel generation can balance and ramp to compensate for renewable intermittency to ensure grid stability. Wind generation above the community electric demand is deemed excess and available to be used by the WR system (Her et al., 2021).

Given computational limitations, optimization is performed for a subset of a year using a procedure developed here to determine representative time periods. Annual renewable resource data were analyzed using k-means algorithms to develop three clusters of weekly patterns per season. The week that best matched the cluster centroid—using root-mean-square error (RMSE) as the metric—was selected. Thus, instead of modeling a full year (8760 h), which exceeded available computation time, the model can optimize over three representative weeks per season (2016 h). The computation time is subsequently reduced to approximately 5 min for the Base Case and several days for the Dispatchability Case. The results are then extrapolated to the 20-year project lifetime.

The FEWMORE model is applied to a remote community in southwestern Alaska without central water infrastructure. The case study community has an existing wind turbine array (~500 kW) with substantial excess generation. The community has interest in solar PV and

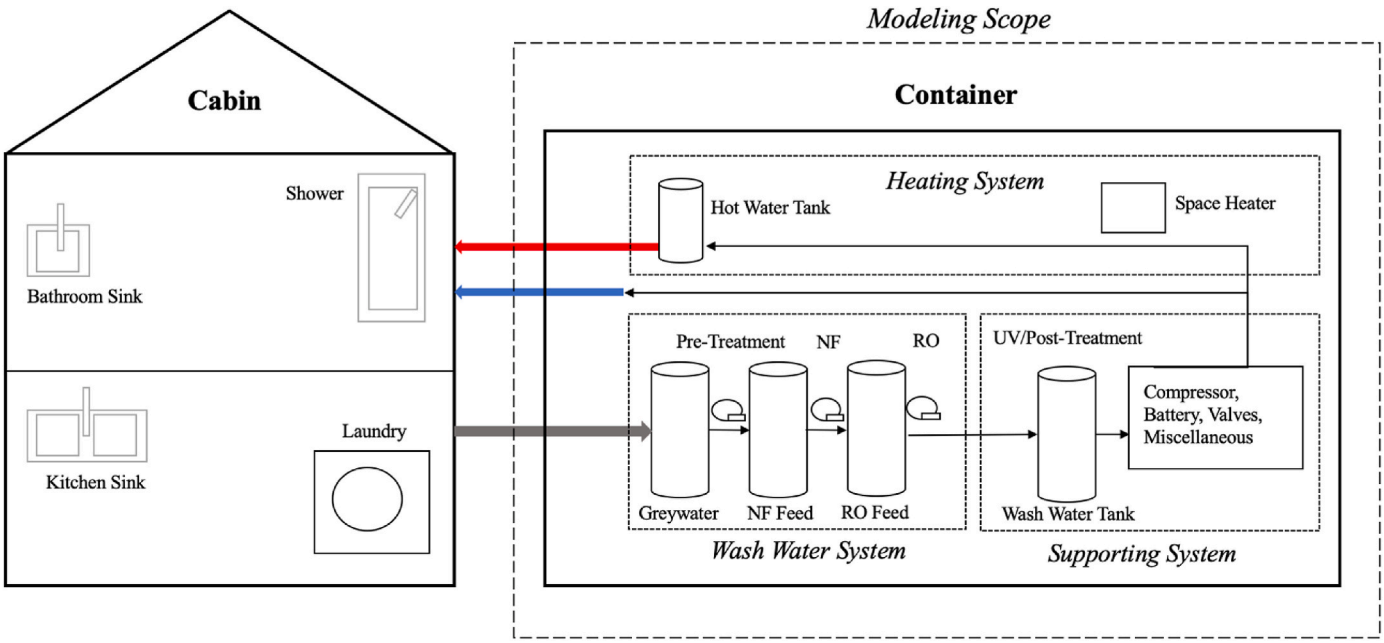

Fig. 4. Experimental set-up of loads and water flows, including the wash-water system technologies and heating system technologies.

new technologies to improve energy and water security. Households currently pay a subsidized electricity rate of $0.45/kWh (Alaska Energy Authority, 2019).

2.4.1. Wash-water system modeling

The CF, NF, and RO processes are considered to be dispatchable, subject to constraints on system operation time and tank capacity. Supporting and miscellaneous processes are not dispatchable, and thus operate as baseload. FEWMORE optimizes how much water CF, NF, and RO should treat per hour, which cannot operate simultaneously. If turned on, a process must treat at least 76 L, excluding rinsing water after shutdown. The greywater and wash-water tanks start with 246 L, and the NF and RO feed tanks begin with 57 L, for a total initial water input of ~600 L. Each tank has a capacity of 341 L (90 gal).

2.4.2. Heating system modeling

An electric 50-L water heater provides hot water for household fixtures. In the Base Case, the thermostat of the tank is set to 52 °C (125 °F). In the Dispatchability Case, the tank thermostat can be controlled within a range of 43–66 °C (110-150 °F). For example, if there is excess renewable energy, the heating element can be dispatched to increase the water temperature. During times of low renewable energy output, water temperature can decline with no heat input until the minimum set point, at which diesel generation would be used. If hot water is demanded, it must be provided at 52 °C.

Power use for water heating results from event-based heat loss and stand-by heat loss. For example, an event occurs when the shower is used, the tank level drops, and water must be replaced and reheated. The heat loss of replacing hot water is dictated by the household demand ($V_{lost,n}$, volume lost in time step n), the volumetric capacitance of water lost (c), and the temperature difference of the hot water leaving (T_{set}) and replacement water (T_{in}), assumed to be the container temperature (see Appendix A). Standby heat loss is determined by the thermal resistance (UA) of the tank and the temperature difference between the stored water (T_n, tank temperature in time step n) and the container interior (T_{in}). Dispatch of electricity to heat is optimally controlled, subject to a finite-difference temperature constraint (Equation (4)).

$$T_{n+1} = T_n + (t/C)*[\eta*Q_{heat} - UA*(T_n - T_{in}) - c*V_{lost,n}*(T_{set} - T_{in})] \quad (4)$$

In addition to the standby heat loss and the amount of heat lost in replacement water, the temperature of the water tank in the future time step ($t = 1$ h) is determined by its temperature in the prior time step, the thermal capacitance of the total water volume (C), and the amount of electric heating dispatched (Q_{heat}, with efficiency $\eta = 100\%$).

Modeling space heating requirements of the container is similar to water heating. However, there is no capacitance effect of replacement water, and stand-by heat loss depends on the temperature difference between the interior and ambient. Heating can be a substantial energy demand and seasonal weather conditions may vary considerably in western Alaska (see Appendix C). No cooling is necessary given mild summers.

2.5. Model simulations

Several model simulations are performed to analyze the effect of dispatching water treatment processes (Dispatchability Case) compared with the control case (Base Case), shown in Table 2. In both the Base and

Table 2
FEWMORE model simulations performed for the control case of no dispatchability (Base Case) and for dispatchable load optimization (Dispatchability Case). Simulations are performed using the wash-water system only as the load and then for the entire WR system load, including water and space heating.

Base Case	Dispatchability Case	Model Notes
Baseline	–	Status quo of running all loads on grid energy (nothing is optimized).
Solar PV	Solar PV	Amount of solar capacity is optimized. In the Dispatchability Case, the amount of water treated per time step is also optimized.
Solar PV & Battery	Solar PV & Battery	Same as above, except battery storage is also allowed to be optimized.
Wind	Wind	Absorption of excess wind energy from the existing community array can be optimized, in addition to solar PV.
–	Water Heating	The water heating system can be dispatched by allowing thermostat settings to be controlled based on solar resource.
–	Water & Space Heating	The water heating and space heating systems can be dispatched by allowing thermostat settings to be controlled, based on both solar and wind resource.

Dispatchability Cases, renewable capacity and dispatch are optimized. The baseline, solar PV, solar PV & battery, and wind simulations are performed twice, first using only the wash-water system as the load and second with the entire WR system demand (wash-water system plus water heating and space heating), in order to compare the DSM potential between water treatment and heating loads. Finally, the water heating and water & space heating simulations are performed for the entire WR system, allowing for dispatchable thermostat settings of heating water and the container.

3. Results and discussion

3.1. Base Case

The Base Case serves as a control analysis in which load dispatch is not optimized and all electric demand is fixed according to the collected load profile. However, solar PV plus battery capacity and dispatch, or excess wind dispatch, can still be optimized. This aims to inform the community how much renewable infrastructure should be added cost-effectively to reduce diesel use for powering the WR system, even if its loads cannot be controlled.

3.1.1. Baseline simulation

First, in the baseline simulation, only the community diesel microgrid (henceforth termed "grid") can power the WR system. This calculates the cost of operating the WR system in the status quo if no renewable energy or load control are added. For the wash-water system demand only (no space or water heating), 3.4 kWh/day are used, translating to a monthly electricity cost of $46/month (see Table 3 for additional results). The total 20-year lifetime cost (or model objective value) of operating the WR system is $11,149. Given this is a relatively substantial cost burden on a household, subsequent simulations determine how adding renewable energy and battery storage may lower costs.

3.1.2. Solar PV simulation

In the solar PV simulation, only solar PV capacity (no battery storage) is optimized. The model determines that a 0.19 kW system (one small panel) is optimal to power the wash-water components of the WR system. In the western Alaska climate, this small solar PV array generates 184 kWh annually. Of the solar generation, 18 kWh are curtailed, given there is no battery storage and the load profile cannot be dispatched. Thus, 166 kWh of diesel generation is displaced, which results in a 13% reduction in grid costs compared to the baseline simulation. The lifetime project cost is reduced by 4%, which is lower than the grid cost reduction because purchasing and installing the solar PV array are included in the lifetime cost.

Overall, adding solar PV to the WR system can be justified for a residence to reduce the cost of water treatment. To be sure, the solar PV array generates unsubstantial amounts of electricity during an arctic winter, and primarily diesel generation is used then. However, solar resource is relatively substantial in the shoulder seasons (late spring and early fall), when snow cover increases ground albedo, and in the summer, when the sun barely sets. Over the course of a year, solar can meet 13% of load. Temporal alignment of generation and load is discussed in Sec. 3.2.

3.1.3. Solar PV and battery simulation

Next, the model can optimize for a battery in addition to solar PV. However, the model determines that battery storage is not cost-effective. Batteries are still quite expensive to purchase, transport, and install in remote arctic regions, especially for small residential systems. Larger, centralized utility-scale installations powering a fleet of WR systems in a community may provide economies of scale; however, the scope of this analysis focuses on a single WR system.

3.1.4. Wind simulation

In the wind simulation, the WR system can use excess wind generation from the existing community wind turbine array. If there is excess wind generation in an hourly period, it is assumed that the WR system can use up to 1 kW of that power, and the model can optimize how much to absorb. The model can still add solar PV capacity, but given that the wind turbine array is existing (no associated capital or operation and maintenance costs), solar PV is not cost-effective if excess wind energy can be used essentially for free.

Wind energy can replace up to 61% of the energy purchased from the grid, compared with the baseline simulation. There is sufficient excess wind energy to power the WR system for 84% of the hours in a year. Thus, there is substantial generation from the community wind array that would otherwise be wasted. This assumes proper controls and frequency regulation of integrating wind with WR systems can be achieved. In reality, there may be additional system integration cost; thus, this simulation models a best-case scenario. Given the scope of this paper is an hourly energy planning tool, optimizing power quality at higher temporal resolution is left to future work.

3.2. Dispatchability Case

In the Dispatchability Case, the CF, NF, and RO processes of the wash-water system can be controlled. The model optimizes when to operate each process and how much water to treat in each hourly time step, subject to the constraints. These results are compared with the Base Case, in order to determine the effect of DSM. Results are presented first considering only the wash-water system demand of the WR system (no heating). Then heating demand is considered, with the hot water tank and electric resistance heater in the container considered as dispatchable loads.

3.2.1. Solar PV simulation

The model determines a 0.45 kW solar PV array (~2 panels) is optimal to power the wash-water system alone. Water treatment DSM reduces grid purchases by 21% and the total lifetime cost by 6%, compared with installing solar PV but no load control (Base Case: solar PV simulation). Thus, optimizing water treatment loads to run on renewables can save over a fifth of diesel use. Dispatching loads also increases solar generation utilization from 13% of load to 27% of load with DSM. Overall, solar PV is a cost-effective investment, including capital, installation, and maintenance costs. Altogether, the effect of installing solar PV and dispatching water treatment loads decreases grid costs by 32%, compared to the status quo (Base Case: baseline simulation). This

Table 3
Optimization results considering the wash-water system demand (no heating) for minimizing total lifetime cost of operating a WR system, in present dollars.

Case	Base				Dispatchability		
Simulation Name	*Baseline*	*Solar PV*	*Battery*	*Wind*	*Solar PV*	*Battery*	*Wind*
Total Lifetime Cost (k$)	11.1	10.7	10.7	4.4	10.1	10.1	3.5
Grid Cost ($/yr)	557	483	483	219	378	378	177
Grid Electricity (MWh/yr)	1.24	1.08	1.08	0.49	0.84	0.84	0.40
Solar PV (kW)	–	0.19	0.19	0	0.45	0.45	0
Renewable Percentage	–	13	13	61	27	27	71

results in a 9% decrease in the total project cost.

3.2.2. Solar PV & battery simulation

When solar PV and battery can be optimized with dispatchable loads, no amount of battery storage is cost-effective. This confirms the hypothesis that battery storage can be reduced or eliminated for the WR system; thus, it is cheaper to store energy as "potential energy" of treated water or thermal energy of heated water, as opposed to electrochemical energy in batteries. For example, treating water requires 4.6 kWh/m^3 and heating water by 1 °C demands 1.2 kWh/m^3. If the initial water input (600 L) is treated according to renewable energy availability for absorbing excess energy, then 2.8 kWh can be "stored" in treated water. Analogously, DSM of container space heating can store 7 kWh (increasing the container temperature and thermal mass of water from 10 to 20 °C, given a specific heat of water of 4.2 kJ/kg-°C). Raising the temperature of the hot water tank within its range (43–66 °C), can store 1.3 kWh. Thus, in theory, 11.1 kWh of renewable generation can be stored rather inexpensively with the setup of DSM sensors and controls. This same amount of battery storage capacity would require at least $22,000 of investment.

3.2.3. Wind simulation

Control of treatment processes and using excess wind energy reduces grid costs by 19%, compared with using excess wind but no load control (Base Case: wind simulation). Total project cost also decreases by 19%, given the existing wind array has no associated capital or maintenance costs. Dispatching loads in coordination with either solar or wind energy both lead to similar proportional cost declines, though wind can meet a larger overall share of the load. Wind can provide up to 71% of wash-water system load compared with 27% for solar PV. Given the high wind resource in western Alaska, dispatching water treatment with wind energy is the most cost-effective choice, assuming proper system integration.

All simulation results for optimizing renewable energy capacity and generation (Base Case) in addition to optimizing renewable energy capacity, generation, and DSM (Dispatchability Case) are presented in Table 3. Thus far, only wash-water system demand has been considered, to allow comparison to other water treatment plants. All other climates are warmer than the Arctic and thus have lower proportional heating demand. Other studies on larger-scale plants in similarly windy, slightly more sunny climates, like northern Europe, have demonstrated similar results; a majority of renewable energy generation is recommended to come from wind, complemented by a smaller amount of solar PV, and batteries are generally not cost-effective (Soshinskaya et al., 2014). No studies have been performed on DSM of small-scale water reuse systems and thus no energy optimization metrics can be compared.

The following analysis includes heating demand, first using fixed thermostat set points for hot water heating and space heating. The prior simulations are rerun using both heating and wash-water system demand (see Table 4). Heating comprises approximately two-thirds of total energy use of the WR system. When heating is included, the optimal solar PV array to meet the demand is approximately doubled, given the higher load.

The energy generation and load profiles for a WR system, powered by an optimal 0.8 kW solar PV array, during a high-resource day in July are shown in Fig. 5. Electricity generation is shown for solar generation meeting baseload power demand (non-dispatchable loads like post-treatment), dispatchable demand of the wash-water (WW) processes, and total demand including heating. Thermostat settings for heating are fixed (no DSM). Any remaining electricity demand not met by solar PV must be provided by the community grid. Any solar generation in excess of total demand is curtailed.

Feed tank levels are displayed in the top half of Fig. 5 to represent the controlled operation of water treatment processes, which are dispatched according to renewable resource availability. In reality, some treatment processes, like RO, may not shut down completely in order to preserve membrane lifetimes, with potentially higher baseload power in practice.

As shown in Fig. 5, water treatment processes are dispatched during daytime periods when solar energy is available. Thus, solar energy can be "stored" by treating water, effectively eliminating the need for a battery. The model dispatches wash-water processes such that pre-treatment raises the NF feed tank level, then NF operates as the NF feed tank decreases and the RO feed tank increases. Finally, RO provides treated water to be stored in the wash-water (WW) tank. The amount of treated water in the WW tank increases throughout the day and then peaks in the late afternoon, then evening household demand reduces this stored water.

Enough treated water is stored to meet the household demand through the next morning, until solar energy is sufficient to begin water treatment. In fact, in the summer, enough energy is provided by the 0.8 kW solar PV array such that the wash-water tank reaches capacity, and some energy must be curtailed.

In Fig. 5, there are two spikes in demand due to heating system operation. The thermostats are set to fixed temperature (no DSM) and thus turn on during the coldest periods late at night and early in the morning. In the following simulations, the heating systems are allowed to be dispatched optimally, using solar PV in Sec. 3.2.4-3.2.5 and wind in Sec. 3.2.6, to determine if the hot water tank and container can instead be heated primarily during times of renewable generation.

3.2.4. Dispatching water heating with solar PV

In the water heating simulation, the temperature set point of the hot water tank can be optimized (the container thermostat for space heating remains fixed). An optimal 1 kW solar PV array with water treatment and water heating dispatch deceases grid costs by 10%, and total lifetime cost by 6%, compared with solar PV and water treatment dispatch without water heating control. Thus, controlling the water heater saves money compared to a fixed temperature set point. The high thermal capacitance of water acts as a good storage medium for storing solar energy until hot water is demanded by the household (demonstrated analogously in Fig. 6).

3.2.5. Dispatching water and space heating with solar PV

Finally, space heating is dispatched, in addition to water heating, by controlling the container thermostat set point. The solar PV array increases to 1.5 kW, 50% higher than the prior water heating simulation. Dispatching the space heater decreases grid costs by 15%, compared with just water heater control. Therefore, dispatching space heating is more effective at reducing grid energy use than water heating alone. The container includes significant thermal mass: in addition to the volume of

Table 4
Optimization results for the entire WR system, including wash-water system and heating demand.

Case	Base			Dispatchability				
Simulation Name	*Baseline*	*Solar PV*	*Wind*	*Solar PV*	*Wind*	*Water Heating*	*Space Heating*	*Wind Heating*
Total Cost (k$)	32.7	32.0	14.2	31.2	12.5	29.4	28.6	7.7
Grid Cost (k$)	1.64	1.48	0.71	1.34	0.62	1.20	1.03	0.39
Grid Energy (MWh/yr)	3.65	3.31	1.59	2.99	1.39	2.68	2.29	0.86
Solar PV (kW)	–	0.41	0	0.82	0	1.0	1.46	0
Renewable Percentage	–	10	70	20	73	31	41	81

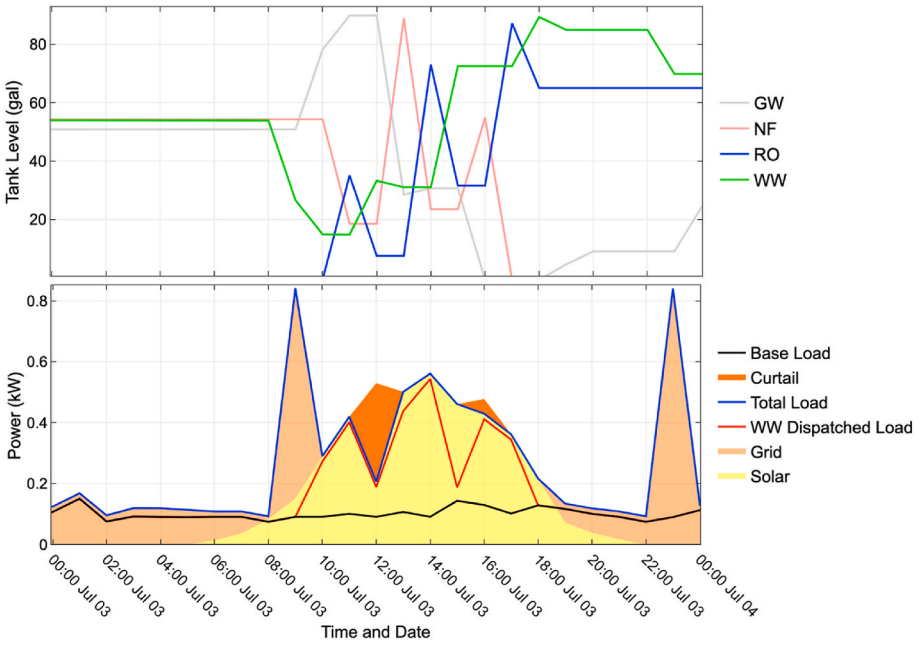

Fig. 5. Feed tank levels (top), demonstrating optimal dispatch of wash-water (WW) processes (CF, NF, and RO), aligned with energy generation and demand profiles (bottom), for a typical summer day. Base Load includes supporting and supplementary processes, while Total Load also includes fixed-thermostat heating systems. Electricity is generated from solar PV or the diesel grid, with excess solar generation curtailed.

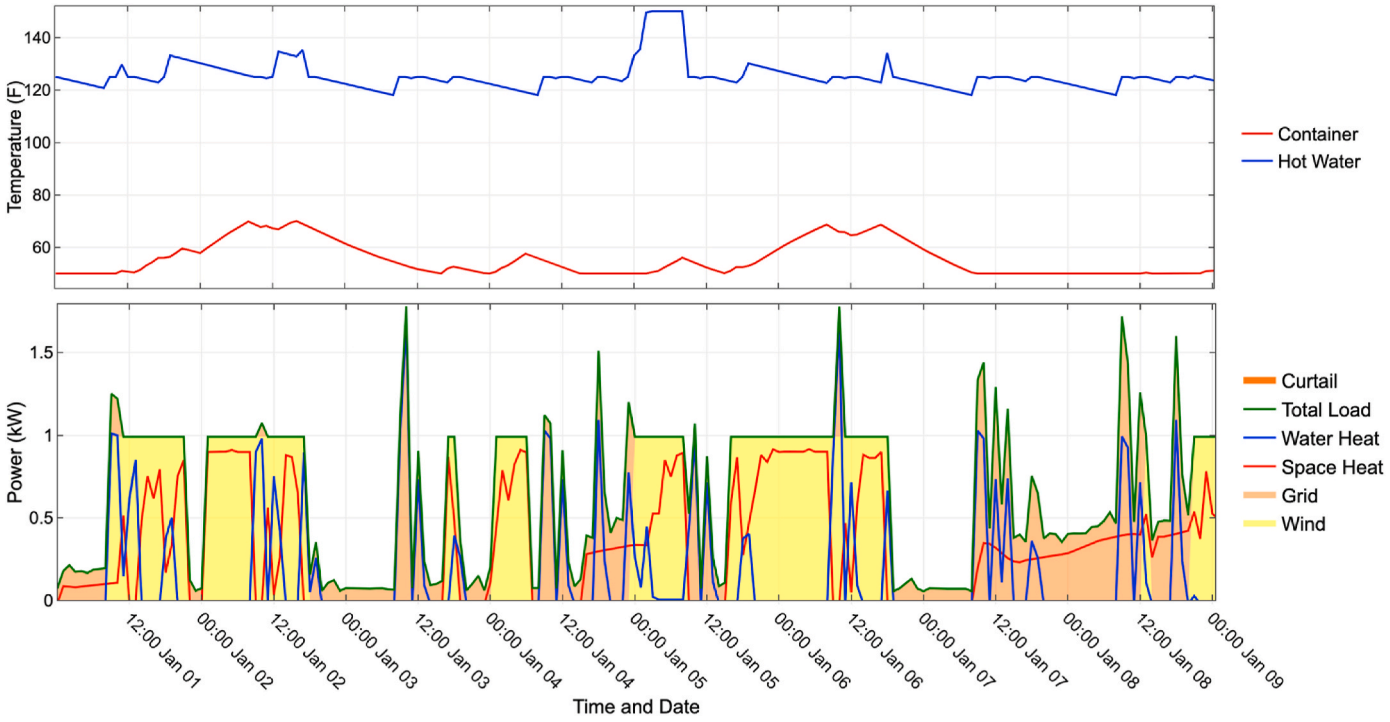

Fig. 6. Change in temperature (top) in the container and the hot water tank, in response to excess wind generation, and WR system electric demand (bottom) over an eight-day period in January. Total Load consists of baseload, dispatchable water treatment, and heating processes.

the hot water tank (50 L), the water treatment feed tanks in the container contribute significant volume (~600 L) of thermal capacitance for modulating the indoor temperature.

Altogether, dispatching heating systems results in substantial savings and increased utilization of renewable energy, compared with fixed thermostat settings. Dispatching both water heating and space heating reduces grid costs by 23%, and total project costs by 9%. Optimizing controls for heating water and the container allows the percent load met by solar PV to increase from 20% to 41%. Thus, when heating is controlled, it can operate more often during periods of solar resource availability; excess solar energy can be used for heating in the late afternoon and stored by increasing the container temperature and associated thermal mass. Then the container temperature can slowly decline through the night until excess renewable energy is available in the morning (see Fig. 6).

FEWMORE aims to inform communities and assist them in making

decisions along the food-energy-water (FEW) nexus to allocate or apply for funding. By adding solar PV, dispatching water treatment, water heating, and space heating, annual diesel use can be reduced by 37% and the total lifetime cost of operating the WR system can be reduced by 13% compared to the status quo. Incorporating the above design decisions would reduce a household's monthly utility payment to power the WR system from $136/month to $85/month with solar PV and load control. The solar PV array could be financed with a shared-savings agreement or grant funded by several programs available for renewable investment in indigenous Alaska communities.

3.2.6. Dispatching water and space heating with wind

Finally, the water and space heating systems can be dispatched to operate on excess wind generation, with diesel generation as needed for grid balancing. Dispatching heating with wind reduces grid costs by 38% compared with just water treatment dispatch. Given the excellent wind resource in western Alaska, the shipping container can be heated during times of high wind generation, with less or no heat needed during periods of low wind. A large acceptable thermostat range and substantial thermal mass allows the temperature to decline slowly if no wind is available. Water thus provides a dual mode of energy storage by modulating changes in temperature, given its high specific heat, and buffering changes in domestic water demand, through ample treated water storage. The effect of using water as thermal mass to moderate changes in temperature is demonstrated in Fig. 6.

As shown in Fig. 6, dispatching heat during times of high excess wind generation can maintain container temperatures above the minimum set point for up to 24 h, without demanding additional heat. For example, the temperature can coast down from mid-afternoon on January 2nd, when the wind stops, to the next period of wind generation. The container temperature can fluctuate over a wide range to accommodate changes in wind energy, given there is no regular human occupation of the container and the main constraint is not freezing pipes. Warmer temperatures in the container also help to improve water treatment operations.

Dispatching water heating in the hot water tank offers less energy storage for load shifting than dispatching space heating in the container. The hot water tank has less than 10% of the thermal mass of the entire shipping container; thus, it declines in temperature more rapidly when wind energy is not available. In practice, it is easier to install and control space heating systems than hot water systems. Modular electric resistance heaters often include programmable thermostats for space heating settings, whereas hot water tanks typically do not offer quantitative water temperature control.

Overall, dispatching all heating optimally allows utilization of wind energy to increase from 73% to 81%. The results of all simulations, considering wash-water and heating demand, are shown in Table 4.

As shown in Table 4, adding solar PV alone without any dispatchability (Base Case: solar PV simulation) reduces total lifetime costs by 3% from the status quo (Base: baseline). Allowing water treatment to be dispatchable (Dispatch: solar PV) yields an additional 5% cost savings; dispatching water heating by another 6%; and dispatching space heating by an additional 10%. Using excess wind generation without dispatchability (Base: wind) reduces total costs by 57% from the status quo. Using excess wind energy while dispatching water treatment (Dispatch: wind) results in 12% more savings, and dispatching heating systems provides 38% additional cost savings. Thus, heating can be a better dispatchable load than water treatment for integrating renewables, especially with wind.

3.2.7. Discussion of sensitivities and limitations

There are several model assumptions on project economics that may impact optimization results. The four most significant model parameters that determine the total lifetime cost of operating the WR system are: the price of grid electricity from the diesel microgrid; the real discount rate associated with the 20-year cash flow analysis of solar PV investment and annual grid purchases; the annual escalation rate of the grid price; and the cost of installing solar PV capacity. The key results of the model are the total lifetime cost to operate the WR system, the optimal amount of solar PV capacity to install, and the amount of energy purchased from the grid (diesel fuel that must be imported).

The price of grid electricity has the most significant impact on model results, as shown in Fig. 7. Among model results, the optimal solar PV capacity varies most with changes in project economics. However, the solar PV array is relatively small (0.4–1.5 kW); thus, the cost of solar PV capacity has an unsubstantial effect on the total lifetime cost. Financing terms of the project are worth careful consideration in order to power the WR system cost effectively over time.

Given constraints on computational time, several assumptions were made that can be studied in future work. Modeling was performed for representative time periods at an hourly resolution, whereas modeling minute resolution may provide a more thorough temporal analysis, albeit with tradeoffs in modeling complexity of water treatment processes.

Additional testing and sensitivity analyses can also be performed, such as varying the initial feed tank water levels, the minimum amount of water required for each process to treat in an operation cycle, and the minimum or maximum time duration between treatment cycles. These experiments can be performed on the prototype to analyze effects on water quality. Wastewater dumps, rinsewater, and backwash processes can also be considered in future modeling.

As with many DSM strategies, sensor and controller integration may be a challenge to dispatching WR system operations. Any additional or existing renewable energy infrastructure would need to have a sensor system that can manage controls of specific water treatment loads, such as reducing water treatment demand when renewable supply is low. Consequently, each feed tank would require a sensor to override controls in case the system is approaching constraints on water quality or tank capacity.

There are many design alternatives that can be addressed in future versions of the WR system. In fact, a new prototype using an aeration process and no protein skimmer is currently in development. The FEWMORE model can also assist in designing optimal capacities of feed tanks in future versions. Different heating systems can be considered as opposed to electric resistance, such as heat pumps or thermal storage with electrothermal stoves, as well is in other areas of the Arctic. Integrating controls with renewable energy systems should be tested and power quality should be studied in future work.

4. Conclusion

An energy optimization model (FEWMORE) utilizing DSM is presented for analyzing a novel WR system as a dispatchable load. The WR system has been designed and constructed to improve energy-water security in a remote Alaska community. Adding 1.5 kW of solar PV and optimally controlling the water treatment and heating processes of the WR system can reduce the lifetime cost—capital, maintenance, and grid costs—by over 13%, and utility bills from the diesel microgrid alone by up to 37%. Another alternative is to power the WR system with excess wind energy from the community wind turbine array, which can decrease total project costs by 68% compared with the status quo. Thus, integrating renewables with the WR system can provide an affordable means of water treatment while also helping to improve energy security and balance energy distribution within the microgrid.

This study is conducted as part of a larger project (MicroFEWs) analyzing the effect of renewable energy on FEW security in remote Alaska communities (Whitney et al., 2019; Chamberlin et al., 2021). The WR system could be delivered and installed in a remote community with solar PV on the roof and grid-tied to the community microgrid or islanded as its own microgrid (See Appendix F). Ongoing implementation of this work is being studied at the Arctic Institute of North America's Kluane Lake Research Station (KLRS) and the University of Calgary,

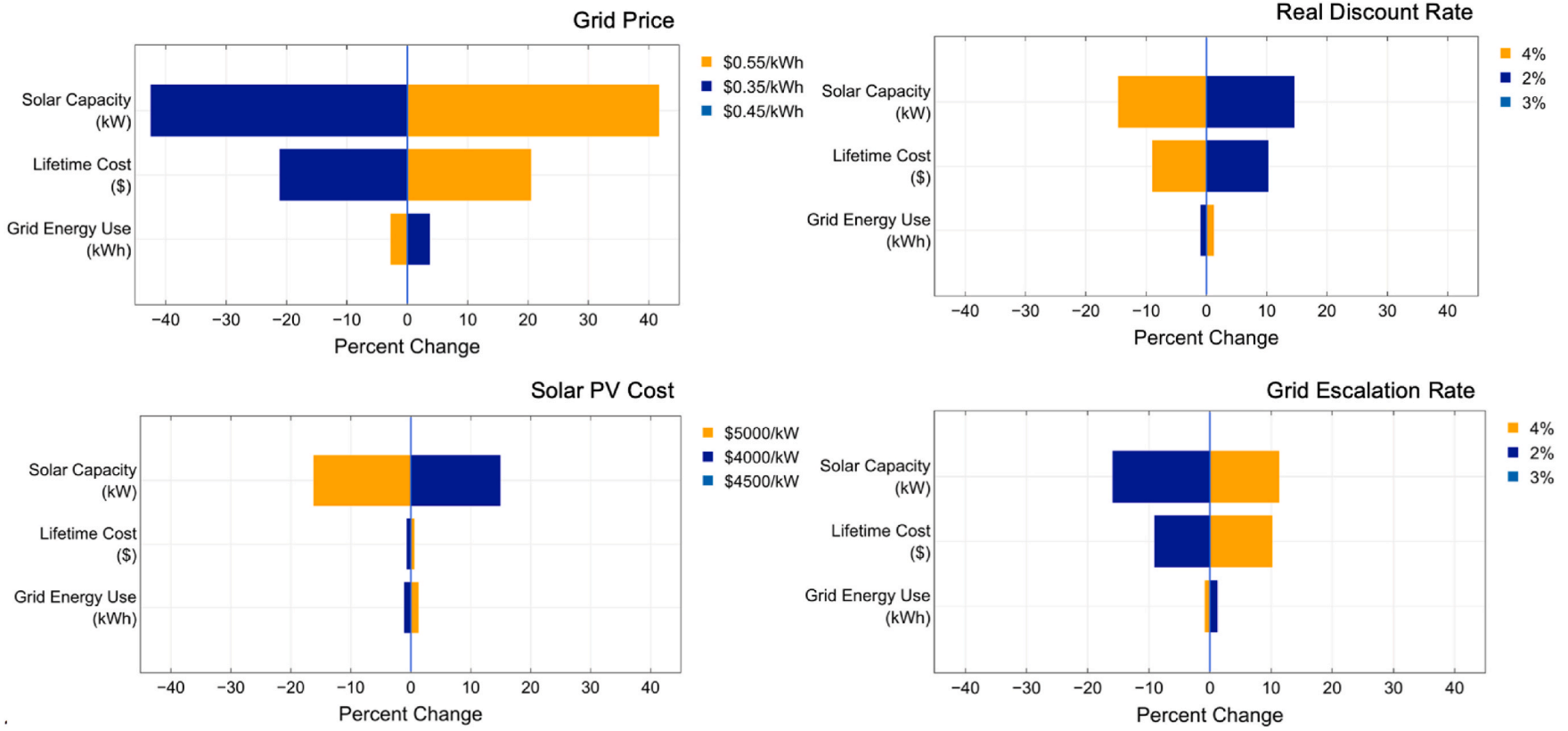

Fig. 7. Sensitivity analysis with regard to price of grid electricity purchased from the diesel microgrid ("grid"), real discount rate of 20-year cash flow analysis, annual grid escalation rate, and solar PV capacity cost.

which are affiliated with this project to test the modeling results in a real microgrid. Experimenting with a WR system integrated with the station's renewable energy system would provide additional insight on the effect that dispatching treatment processes and fluctuating water temperatures have on water quality, membrane lifetimes, and overall energy use.

Over the past year at KLRS, sensor and data collection systems have been deployed for the microgrid as a prerequisite to DSM strategies. A cabin has been selected for water system installations and DSM testing, given it houses scientists who are amenable to experimentation of its water services. A modular sewage treatment system has also recently been installed to test similar water treatment operations on the microgrid before the WR system prototype is available for installation. Managing the procurement, transportation, and installation of a new WR system will require sophisticated project management, though recent experience of installing the sewage treatment system has shown that such a project would be feasible at KLRS.

Human-based trials of the WR system are currently in the first of a two-phase process prior to consideration of field implementation. A UAA dormitory has been retrofitted to have this system installed (with technological modifications not previously shown) and will begin testing shortly. This testing will target assessment of system efficacy with human-generated greywater quality and flow patterns, as well as subsequent assessment of aesthetic reused water quality and user-based system maintenance. Through this testing and ongoing discussions with the State of Alaska, subsequent phases will be developed to include development of management tools, such as potential a state-wide maintenance cooperative.

The issues of energy and water security in off-grid communities are not only applicable in Alaska and the Arctic; similar conditions exist throughout the developing world. The FEWMORE model can be applied to study the integration of other regionally-appropriate water treatment and renewable energy systems, based on local preferences along the energy-water nexus.

Funding

This research was funded by the United States National Science Foundation, Award #1740075: "INFEWS/T3: Coupling infrastructure improvements to food-energy-water system dynamics in small cold region communities: MicroFEWs."

CRediT authorship contribution statement

Daniel J. Sambor: Conceptualization, Methodology, Software, Validation, Formal analysis, Data curation, Writing – original draft, Preparation, Writing – review & editing, Visualization. **Samantha C.M. Bishop:** Methodology, Validation, Formal analysis, Data curation, Writing – review & editing, Visualization. **Aaron Dotson:** Conceptualization, Methodology, Investigation, Data curation, Writing – review & editing, Supervision, Project administration, Funding acquisition. **Srijan Aggarwal:** Conceptualization, Methodology, Investigation, Writing – review & editing, Supervision, Project administration, Funding acquisition. **Mark Z. Jacobson:** Writing – review & editing, Supervision.

Declaration of competing interest

The authors declare that they have no known competing financial interests or personal relationships that could have appeared to influence the work reported in this paper.

Acknowledgments

The authors would like to acknowledge Joe Selmont, Erin Whitney, Barbara Johnson, Harry Penn, and the MicroFEWs group for their support and revisions.

Appendix A. Model Inputs

A.1. Time Series Inputs

- Electric load profile of WR system *(l_t) [*kW average in each hour: kWh*]*
- Domestic water demand profile *[*L*]*
- Excess wind energy profile *[*kWh*]*
- Ambient temperature profile *($T_{amb,t}$) [*^{o}C*]*
- Solar yield profile *(s_t) [*kW_{AC} in each hour per kWp_{DC} installed, includes losses*]*

A.2. Hot Water Heating

- Tank diameter = 0.46 m
- Tank height = 0.61 m
- Tank R-value = 9.1 m^2-^{o}C/W (16 hr-ft^2-^{o}F/Btu)
- Tank volume = 50 L
- Volumetric capacitance of water: c = 0.36 Wh/L-^{o}C (62.4 Btu/ft^3-^{o}F)

A.3. Economic Inputs

- Grid price (unsubsidized): C_G = $0.45/kWh
- Project lifetime: y = 20 years (lifetime of all equipment, except for 10-yr battery lifetime)
- Real discount rate = 3%
- Real grid escalation rate = 3%
- Solar PV capacity cost (installed): C_S = $4500/kW
- Solar PV operation & maintenance (O&M) cost: O_S = $50/kW/yr
- Capacity cost of battery inverter (installed): C_I = $1000/kW
- Capacity cost of battery storage (installed): C_E = $1000/kWh
- Battery variable O&M cost: $0.005/$kWh_{throughput}$
- Battery fixed O&M cost: $30/kW/yr

A.4. Technology Inputs

- Battery round-trip efficiency: 90%
- Battery depth-of-discharge: $DOD = 80\%$
- Battery self-discharge rate: $SD = 0.01\%/hr$
- Container dimensions: 2.4 m × 2.6 m x 3 m (8 ft × 8.5 ft x 10 ft)
- Container R-value = 10.3 m^2-°C/W (18 hr-ft^2-°F/Btu)
- Electric resistance heating efficiency = 100%

A.5. Model Outputs

- Capacity planning:
- Capacity of solar PV array [kW]
- Capacity of battery storage [kWh]
- Capacity of battery inverter [kW]
- Dispatch scheduling:
- Time series of solar output [kWh]
- Time series of solar curtailment [kWh]
- Time series of excess wind absorption [kWh]
- Time series of grid purchases [kWh]
- Time series of battery charging/discharging [kWh]
- Time series of dispatchable load demand [kWh]
- Total energy output:
- Amount of grid electricity consumed [kWh/yr]
- Amount of solar electricity generated and curtailed [kWh/yr]
- Total project costs (objective value):
- Total cost of installing and maintaining solar PV system
- Total cost of installing, maintaining, and replacing battery storage system
- Total cost of grid electricity purchased

Appendix B. Model Condensed Mathematical Form

B.1. Decision Variables

- Amount of solar PV capacity to install *(S)* [kW]
- Amount of battery storage capacity to install *(E)* [kWh]
- Amount of battery inverter capacity to install *(I)* [kW]
- Amount of excess wind energy to absorb *(W)* [kWh]
- Dispatch time series of battery storage (charge and discharge*)* ($E_{t,\ in/out}$) [kWh]
- Dispatch time series of solar electricity curtailment (R_t) [kWh]
- Dispatch time series of grid electricity purchases (G_t) [kWh]
- Dispatch time series of space heating system ($Q_{t,heat}$) [kWh]
- Dispatch time series of water heating system ($Q_{t,water}$) [kWh]

B.2. Objective

- Minimize total project costs of water reuse energy operations over lifetime:

$$\min \Sigma_t\ C_g{*}G_t + S{*}C_s + C_E{*}E + C_I{*}I \tag{B1}$$

where the summation is over all hourly time steps, *t*, of the representative time period, which is extrapolated over the 20-year lifetime as part of a discounted cash flow. *C* is the cost of each component (including initial capital cost plus total lifetime operating cost), where *g* is grid electricity, *s* is solar PV array capacity, *E* is the battery energy storage capacity, and *I* is the inverter capacity.

B.3. Defined variables

- Current amount of energy stored in battery storage:

$$SE_{t+1} = SD{*}[c{*}E_{in,t} - (1/d){*} + E_{out,t}] \tag{B2}$$

Where c and d are the charging and discharging efficiencies, respectively, together resulting in a round-trip efficiency of 90%, and SD is the self-discharge rate.

- Temperature of hot water tank:

$$T_{t+1} = T_t + (1/C){*}[\eta{*}Q_{heat} - UA{*}(T_t - T_{in}) - c{*}V_{lost,t}{*}(T_{set} - T_{in})] \tag{B3}$$

Where *C* is the thermal capacitance (Wh/°C) of the water stored in the tank when full, defined as the product of the volumetric capacitance of

water, c, and the tank volume. The efficiency (η) of electric resistance heating is assumed to be 100%. The stand-by heat loss from the container is defined by its thermal resistance (UA, product of U-value—inverse of R-value—and tank surface area) multiplied by the temperature difference between the water in the tank and the interior temperature of the container (T_{in}, which is set at a minimum of 10 °C). Finally, the effect of reducing the temperature of the tank by removing an amount of hot water demanded by the house (V_{lost} in time step t) at the desired temperature ($T_{set} = 52$ °C) is calculated based on the volumetric capacitance of water and the temperature difference compared to incoming water (assumed to be at the container interior temperature).

· Temperature of the container interior:

$$T_{t+1} = T_t + (1/C)*[\eta*Q_{heat} - UA*(T_t - T_{amb})] \quad \text{(B3)}$$

Where C is the thermal capacitance (Wh/°C) of the container, assumed to be dominated by the thermal capacitance of the water stored in all treatment process feed tanks inside the container (~600 L). The stand-by heat loss is determined by the heat loss coefficient of the container envelope (UA) and the temperature difference between the interior and the ambient.

B.4. Constraints

· Overall electricity flows must be balanced in each time step:

$$G_t + S_t + W_t + E_{out,t} = l_t + E_{in,t} + R_t \quad \text{(B3)}$$

where the electric load demand (l_t) is composed of both baseload demand and total dispatchable load demand from the wash-water system and heating system.

· Battery storage state of charge must lie within limits *[kWh]*, given an initial state of charge of 0%:

$$0 < SE_t < DOD*E \quad \text{(B4)}$$

· Battery charging/discharging cannot exceed power requirements of inverter *[kW]:*

$$0 < E_{in/out,t} < I \quad \text{(B5)}$$

Sensible thermal energy must be balanced across container envelope at all times:

$$Q_{heat,t} = Q_{cond,t} \quad \text{(B6)}$$

where $Q_{cond,t}$ is the heat loss due to conduction through the container envelope, given its thermal resistance (See Appendix C).

· Water stored in each feed tank must be less than its capacity of 341 L (90 gal).
· Each water treatment process can recycle 76 L (20 gal) per cycle.
· Only one treatment process can operate at a time.
· Greywater and wash-water feed tanks are initialized at 246 L.
· NF and RO feed tanks are initialized at 57 L.

Appendix C. Container Energy Modeling

Heat is transferred via conduction between the interior of the container, through its envelope, and the ambient environment. Given the Arctic climate, heat is transferred from the container interior ($T_{int,t}$) to the cold outdoors ($T_{amb,t}$) during the vast majority of the year. The subsequent heat lost from the container is defined as:

$$Q_{cond,t} = U\,A\,(T_{int,t} - T_{amb,t}). \quad \text{(C1)}$$

The units of heat flows, Q, are in watts of thermal power *(W)* and, given that the thermal power is an average value over the 1-h time step, it is equivalent to the amount of thermal energy in each hour *(Wh)*. No cooling is assumed to be required in the summer, given the cold climate, and thus no maximum temperature in the container is preset.

Appendix D. Water Reuse System Energy Modeling

Within an hourly temporal resolution there are fluctuations in the energy use of the water treatment processes. Most processes have constant power draw, except for RO, which decreases initially as the water warms up, then plateaus, and finally increases as concentration increases. The mean power is 0.41 kW. The initial period is weighted by a factor of 2 and the final period by a factor of 3, which yields an average power of 0.42 kW. The power draw is shown in Figure D1.

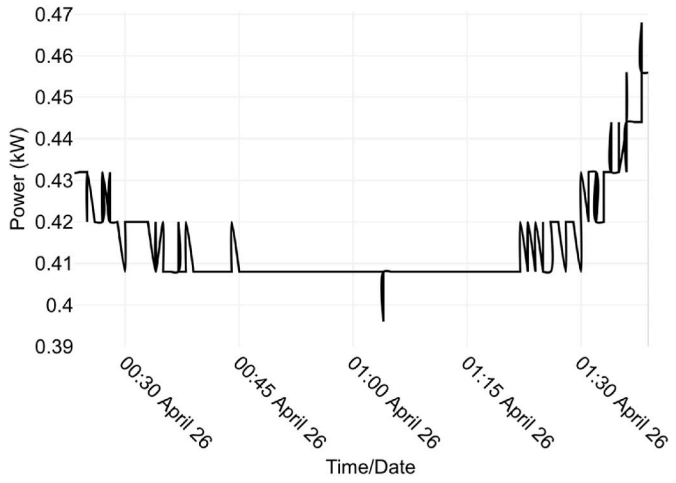

Fig. D1. Power draw of a reverse osmosis cycle by minute over an approximately 1.5-h treatment time period.

Appendix E. Water Reuse System Components

The specifications of the components of the wash-water system within the Water Reuse system are shown in Table E1.

Table E1
Details of select wash-water system components of the WR system.

Part	Size	Model	Flow Rate (L/hr)	Power (W)
Protein skimmer	250 mm	Skimz Monzter SM253 DC	1200–2400	40
Greywater Tank	341 L	–	–	–
Membrane Pump	–	Procon 113B015F31 B	2725	200–400
Cartridge Filter	1 μm	–	1135	–
Cartridge Filter	0.45 μm	–	1135	–
Cartridge Filter	0.2 μm	–	1135	–
NF Feed Tank	341 L	–	–	–
NF	7.6 m^2	DOW Filmtec NF 270	2725	–
RO Feed Tank	341 L	–	–	–
RO	8.7 m^2	DOW Filmtec LE LC 4040	2725	–
UV	1590 L/h	Viqua VH200	170	35
Ozone	–	Viqua S2Q-OZ UV	–	22

Appendix F. Solar PV Integration

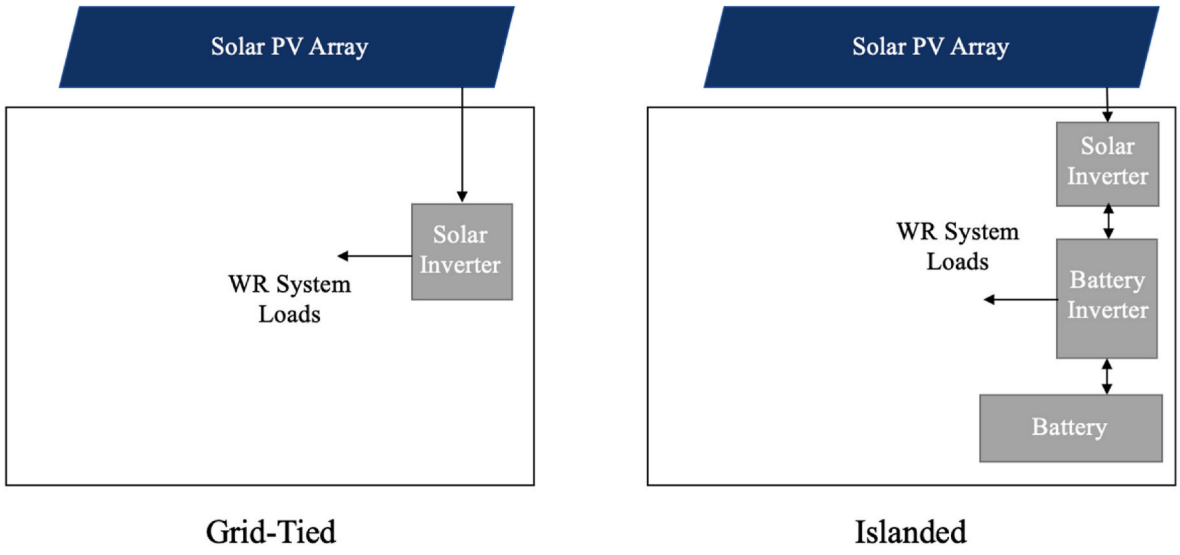

Fig. F1. Schematic of Solar PV integration of Water Reuse system and community microgrid (left), and islanded as its own microgrid (right).

References

Aghajani, G.R., Shayanfar, H.A., Shayeghi, H., 2017. Demand side management in a smart micro-grid in the presence of renewable generation and demand response. Energy 126, 622–637.

Alaska Energy Authority, 2019. Power Cost Equalization Program. Statistical Report.

Chamberlin, M.J., Sambor, D.J., Karenzi, J., Wies, R., Whitney, E., 2021. Energy distribution modeling for assessment and optimal distribution of sustainable energy for on-grid food, energy, and water systems in remote microgrids. Sustain. Times 13 (17), 9511. https://doi.org/10.3390/SU13179511.

Dieter, C.A., Maupin, M.A., Caldwell, R.R., Harris, M.A., Ivahnenko, T.I., Lovelace, J.K., Barber, N.L., Linsey, K.S., 2018. Estimated use of water in the United States in 2015. US Geol. Surv. Circular 1441, 1–65. https://doi.org/10.3133/cir1441.

Dotson, A.D., 2017. Alaska Water and Sewer Challenge: Phase 3 - Final Report.

Dunning, I., Huchette, J., Lubin, M., 2017. JuMP: a modeling language for mathematical optimization. SIAM Rev. 59.2, 295–320.

Eichelberger, L.P., 2010. Living in utility scarcity: energy and water insecurity in Northwest Alaska. Publ. Health 100, 1010–1018. https://doi.org/10.2105/AJPH.2009.160846.

Eichelberger, L., Hickel, K., Thomas, T.K., 2020. A community approach to promote household water security: combining centralized and decentralized access in remote Alaskan communities. Water Secur 10, 100066. https://doi.org/10.1016/j.wasec.2020.100066.

Emami, N., Sobhani, R., Rosso, D., 2018. Diurnal variations of the energy intensity and associated greenhouse gas emissions for activated sludge processes. Water Sci. Technol. 7 https://doi.org/10.2166/wst.2018.054.

Gude, V.G., 2015. Energy and water autarky of wastewater treatment and power generation systems. In: Renewable and Sustainable Energy Reviews. Elsevier, pp. 52–68. https://doi.org/10.1016/j.rser.2015.01.055.

Hennessy, T.W., Bressler, J.M., 2016. Improving Health in the arctic region through safe and affordable access to household running water and sewer services: an arctic council initiative. Int. J. Circumpolar Health, 31149. https://doi.org/10.3402/ijch.v75.31149.

Hennessy, T.W., Ritter, T., Holman, R.C., Bruden, D.L., Yorita, K.L., Bulkow, L., Cheek, J. E., Singleton, R.J., Smith, J., 2008. The relationship between in-home water service and the risk of respiratory tract, skin, and gastrointestinal tract infections among rural Alaska natives. Am. J. Publ. Health 98 (11), 2072–2078. https://doi.org/10.2105/AJPH.2007.115618.

Her, C., Sambor, D.J., Whitney, E., Wies, R., 2021. Novel wind resource assessment and demand flexibility analysis for community resilience: a remote microgrid case study. Renew. Energy 179, 1472–1486. https://doi.org/10.1016/J.RENENE.2021.07.099.

Hickel, K.A., Dotson, A., Thomas, T.K., Heavener, M., Hébert, J., Warren, J.A., 2018. The search for an alternative to piped water and sewer systems in the Alaskan Arctic. Environ. Sci. Pollut. Res. 25 (33), 32873–32880. https://doi.org/10.1007/s11356-017-8815-x.

Holdmann, G.P., Wies, R.W., Vandermeer, J.B., 2019. Renewable energy integration in Alaska's remote islanded microgrids: economic drivers, technical strategies, technological niche development, and policy implications. Proc. IEEE 107 (9), 1820–1837. https://doi.org/10.1109/JPROC.2019.2932755.

Jabir, H., Teh, J., Ishak, D., Abunima, H., 2018. Impacts of demand-side management on electrical power systems: a review. Energies 11 (5). https://doi.org/10.3390/en11051050.

Khan, M.F., Pervez, A., Modibbo, U.M., Chauhan, J., Ali, I., 2021. Flexible fuzzy goal programming approach in optimal mix of power generation for socio-economic sustainability: a case study. Sustainability 13 (15), 8256. https://doi.org/10.3390/su13158256.

Kirchem, D., Lynch, M., Bertsch, V., Casey, E., 2020. Modelling demand response with process models and energy systems models: potential applications for wastewater treatment within the energy-water nexus. Appl. Energy. https://doi.org/10.1016/j.apenergy.2019.114321.

Lucas, C., Johnson, B., Hodges Snyder, E., Aggarwal, S., Dotson, A., 2021. A tale of two communities: adopting and paying for an in-home non-potable water reuse system in rural Alaska. ACS ES&T Water 1 (8), 1807–1815.

Michaelson, G., 2017. Development of a Physicochemical Greywater Reuse Treatment System for Intentional Human Contact. Diss. University of Alaska Anchorage.

Moura, P.S., De Almeida, A.T., 2010. The role of demand-side management in the grid integration of wind power. Appl. Energy 87, 2581–2588.

Moura, P.S., de Almeida, A.T., 2010. Multi-objective optimization of a mixed renewable system with demand-side management. Renew. Sustain. Energy Rev. 1461–1468. https://doi.org/10.1016/j.rser.2010.01.004.

Neves, D., Pina, A., Silva, C.A., 2015. Demand response modeling: a comparison between tools. Appl. Energy 146, 288–297. https://doi.org/10.1016/j.apenergy.2015.02.057.

NSF International, 2019. NSF 350-2018: onsite residential and commercial water reuse treatment systems. STANDARD NSF International. https://www.techstreet.com/nsf/standards/nsf-350-2018?product_id=2044416. (Accessed 10 February 2021).

Penn, H.J.F., Loring, P.A., Schnabel, W.E., 2017. Diagnosing water security in the rural North with an environmental security framework. J. Environ. Manag. 199, 91–98. https://doi.org/10.1016/j.jenvman.2017.04.088.

Pina, A., Silva, C., Ferrão, P., 2012. The impact of demand side management strategies in the penetration of renewable electricity. Energy 41 (1), 128–137. https://doi.org/10.1016/j.energy.2011.06.013.

Pourmousavi, S.A., Nehrir, M.H., Patrick, S.N., 2014. Real-time demand response through aggregate electric water heaters for load shifting and balancing wind generation. IEEE Trans. Smart Grid 5 (2), 769–778. https://doi.org/10.1109/TSG.2013.2290084.

Quitoras, M.R.D., 2020. Holistic and Integrated Energy System Optimization in Reducing Diesel Dependence of Canadian Remote Arctic Communities. Thesis.

Quitoras, M.R., Campana, P.E., Crawford, C., 2020. Exploring electricity generation alternatives for Canadian arctic communities using a multi-objective genetic algorithm approach. Energy Convers. Manag. 210, 112471 https://doi.org/10.1016/j.enconman.2020.112471.

Rashedin, M., Dev, S., Whitney, E., Madden, D., Aggarwal, S., 2020. Energy consumption for domestic water treatment and distribution in remote Alaskan communities. In: Poster Presented at AGU Conference. https://doi.org/10.13140/RG.2.2.22871.09124. San Francisco, CA.

Rezaei, N., Kalantar, M., 2015. Smart microgrid hierarchical frequency control ancillary service provision based on virtual inertia concept: an integrated demand response and droop controlled distributed generation framework. Energy Conv. Manag. (92), 287–301.

Sambor, D., Wilber, M., Whitney, E., Jacobson, M., 2020. Development of a tool for optimizing solar and battery storage for container farming in a remote Arctic microgrid. Energies 13 (19), 5143. https://doi.org/10.3390/en13195143.

Soshinskaya, M., Crijns-Graus, W.H.J., van der Meer, J., Guerrero, J.M., 2014. Application of a microgrid with renewables for a water treatment plant. Appl. Energy 134, 20–34. https://doi.org/10.1016/j.apenergy.2014.07.097.

United States Arctic Research Commission Alaska Rural Water and Sanitation Working Group, 2015. Alaskan Water and Sanitation Retrospective.

U.S. Energy Information Administration, 2020. Monthly Electric Power Industry Report: Form EIA-861M.

Whitney, E., Schnabel, W.E., Aggarwal, S., Huang, D., Wies, R.W., Karenzi, J., Huntington, H.P., Schmidt, J.I., Dotson, A.D., 2019. MicroFEWs: a food–energy–water systems approach to renewable energy decisions in islanded microgrid communities in rural Alaska. Environ. Eng. Sci. 36 (7), 843–849. https://doi.org/10.1089/ees.2019.0055.

Zia, M.F., Elbouchikhi, E., Benbouzid, M., 2018. Microgrids energy management systems: a critical review on methods, solutions, and prospects. Appl. Energy 222, 1033–1055. https://doi.org/10.1016/j.apenergy.2018.04.103.

Zohrabian, A., Sanders, K.T., 2020. The energy trade-offs of transitioning to a locally sourced water supply portfolio in the city of Los Angeles. Energies 13 (21), 5589. https://doi.org/10.3390/en13215589.